The International Supercritical CO_2 Energy Technologies Symposium
March 2 - 5, 2026, Pittsburgh, PA
Paper #55

Technoeconomic Analysis of sCO_2 Power Cycles Integrated in a Particle-based CSP System Exploring the Influence of Design Parameters at Different Turbine Inlet Temperatures

Taylor Brown
Thermal Systems R&D Group
National Laboratory of the Rockies
Golden, CO, USA

Ty Neises
Thermal Systems R&D Group
National Laboratory of the Rockies
Golden, CO, USA

William Hamilton
Thermal Systems R&D Group
National Laboratory of the Rockies
Golden, CO, USA

Taylor is a researcher in the Thermal Energy Systems group at NLR, with a background in mechanical engineering. His research focuses on modeling concentrating solar power systems, thermal energy storage, and sCO_2 power cycles. He is a member of the System Advisor Model (SAM) and SolTrace development teams.

Ty is a senior researcher in the Thermal Systems group at NLR where he focuses on techno-economic analysis of thermal energy systems. Ty leads development of thermal technology models in NLR's System Advisor Model (SAM). Ty's sCO_2 research focuses on developing models to understand the integration of sCO_2 cycles with solar thermal and thermal energy storage.

William (Bill) Hamilton joined the Thermal Sciences Group at NLR in 2019. His work at NLR includes the development of models to evaluate and optimize the performance, design, and dispatch of concentrating solar power energy systems. Bill contributes to many NLR open-source software tools including SolTrace, SolarPILOT, and System Advisor Model (SAM). His research experience is in the fields of thermal system modeling, deterministic mixed-integer programming, and CSP system design using derivative-free optimization algorithms.

ABSTRACT

In this work, we compare the technoeconomic performance of four supercritical carbon dioxide (sCO_2) power cycle configurations – simple with bypass, recompression with bypass, partial cooling, and turbine split flow – integrated in a system level design point particle-based CSP model. The CSP system is comprised of a falling particle receiver heating particles to 775 °C, two tank particle storage, and a heliostat field designed by SolarPILOT. We calculate the system specific cost to quantify the performance of each cycle design. To understand how the design-point turbine inlet temperature influences system techno-economic performance under different assumptions, we perform a sensitivity study that varies key cycle and system level parameters, as well as various component cost models, for turbine inlet temperatures of 550, 625, and 700 °C. For each inlet temperature, we vary the turbomachinery isentropic efficiencies and primary heat exchanger (PHX) cold approach temperatures, along with the cost of the heliostats, PHX, recuperators, and thermal energy storage. Initial results show that colder turbine inlet temperatures have better technoeconomic performance, due to the cost savings in the turbine and primary heat exchanger, which overcome the cost penalty resulting from decreased cycle thermal efficiency. The analysis demonstrates how the cycle design philosophy is impacted by these variations.

INTRODUCTION

Supercritical carbon dioxide (sCO_2) power cycles are a promising option for next generation concentrating solar power (CSP) systems due to their high thermal efficiency, compact turbomachinery, and strong performance at small and large scales. Additionally, sCO_2 cycles can take advantage of sensible heat rejection to manage air cooler costs in the arid environments common for CSP installations [1].

Next generation CSP (Gen3) systems aim to achieve higher solar to electric conversion efficiencies by targeting heat transfer fluid temperatures (HTF) hotter than 700 °C. Solid particles are being explored as a Gen3 HTF because they are a low-cost material that is stable at a wide range of temperatures. In this paper, we are modeling the falling particle receiver under development at Sandia National Laboratories [2] that directly irradiates particles at the top of the power tower via a solar field of heliostat mirrors that concentrate thermal radiation from the sun. The particles collect heat and then either travel directly to the power cycle's primary heat exchanger (PHX) to transfer heat to the sCO_2, or to direct thermal energy storage (TES) tanks to be dispatched later.

CSP systems balance three main characteristics of the power cycle which affect the system design: cycle thermal efficiency, HTF temperature difference across the heat input, and cycle cost. Higher thermal efficiencies require less heat from the CSP system to achieve the same target power output, which reduces the size and cost of the solar field, tower, receiver, and TES. Larger HTF temperature differences reduce the size of the TES, as less HTF mass is required to store the same amount of energy, thereby reducing TES cost. Thermal efficiency and HTF temperature difference are often inversely related, as cycles with higher efficiency tend to have more recuperation, which decreases the cold approach temperature at the PHX. Similarly, cycle costs tend to rise with thermal efficiency, as the cost of the recuperators rise as the conductance increases.

We compared the performance of multiple sCO_2 cycle configurations integrated in a falling particle CSP system in a recent work [3]. We performed a parametric sweep of cycle free parameters, such as minimum pressure, flow fractions, and recuperator conductance, for each configuration and used the resulting cycle efficiency, HTF temperatures, and cost as inputs into a CSP system model. The full system model produced the system specific cost (SSC), which is

the total installed cost divided by the cycle net power, including parasitics. For the 'baseline' analysis, we assumed a fixed turbine inlet temperature (TIT) of 700 °C and hot particle temperature of 775 °C. Following the baseline study, we also performed a sensitivity analysis, which included decreasing the turbine inlet temperature to 625 °C and 550 °C. These reduced temperature scenarios performed better than the baseline 700 °C, significantly reducing the SSC. The colder turbine inlet temperatures decreased the cost of the turbine and high temperature recuperator due to high temperature material costs, decreased the PHX cost by increasing the hot approach temperature, and decreased the TES costs by increasing the HTF temperature difference. Conversely, the cycle efficiency decreased, which increased the cost of the solar field, tower, and receiver, but this difference was overcome by the other cost savings.

Other researchers have also analyzed the effect of the turbine inlet temperature on the techno-economic performance of particle CSP systems. Alfani et al. [4] modeled a 20 MW net electric CSP system with a tubular fluidized particle receiver, comparing the recompression cycle with optional intercooling or HTR bypass, and partial cooling cycle configurations. They varied the HTF hot temperature into the PHX and sCO_2 turbine inlet temperature. The maximum HTF temperature produced the best performance, while the turbine inlet temperature was optimal around 660-720 °C depending on the configuration, which was between the bounds of their analysis, 600-740 °C.

Heller et al. studied the design point [5] and off-design [6] techno-economic performance of a 115 MWe particle CSP system with centrifugal receivers. They modeled the simple, recompression, and partial cooling cycles all with and without reheating and intercooling. They used a fixed HTF hot temperature of 900 °C, and varied the turbine inlet temperature from 550-700 °C. The colder turbine inlet temperatures were optimal, saving cost in the turbine and recuperators from the lower operating temperature, and reduced the cost of the PHX due to the larger approach temperatures.

In this work, we expand our sensitivity study presented in our prior work [3], to focus on system performance at colder turbine inlet temperatures. We vary key system parameters, such as the PHX cold approach temperature and turbomachinery isentropic efficiency, along with various system cost models to understand their effect on system performance and optimal cycle design philosophy.

METHODOLOGY

The sCO_2 power cycle models, CSP system model, and parametric sweep methodology are detailed in our recent work, Brown et al. [3], and key characteristics are summarized below.

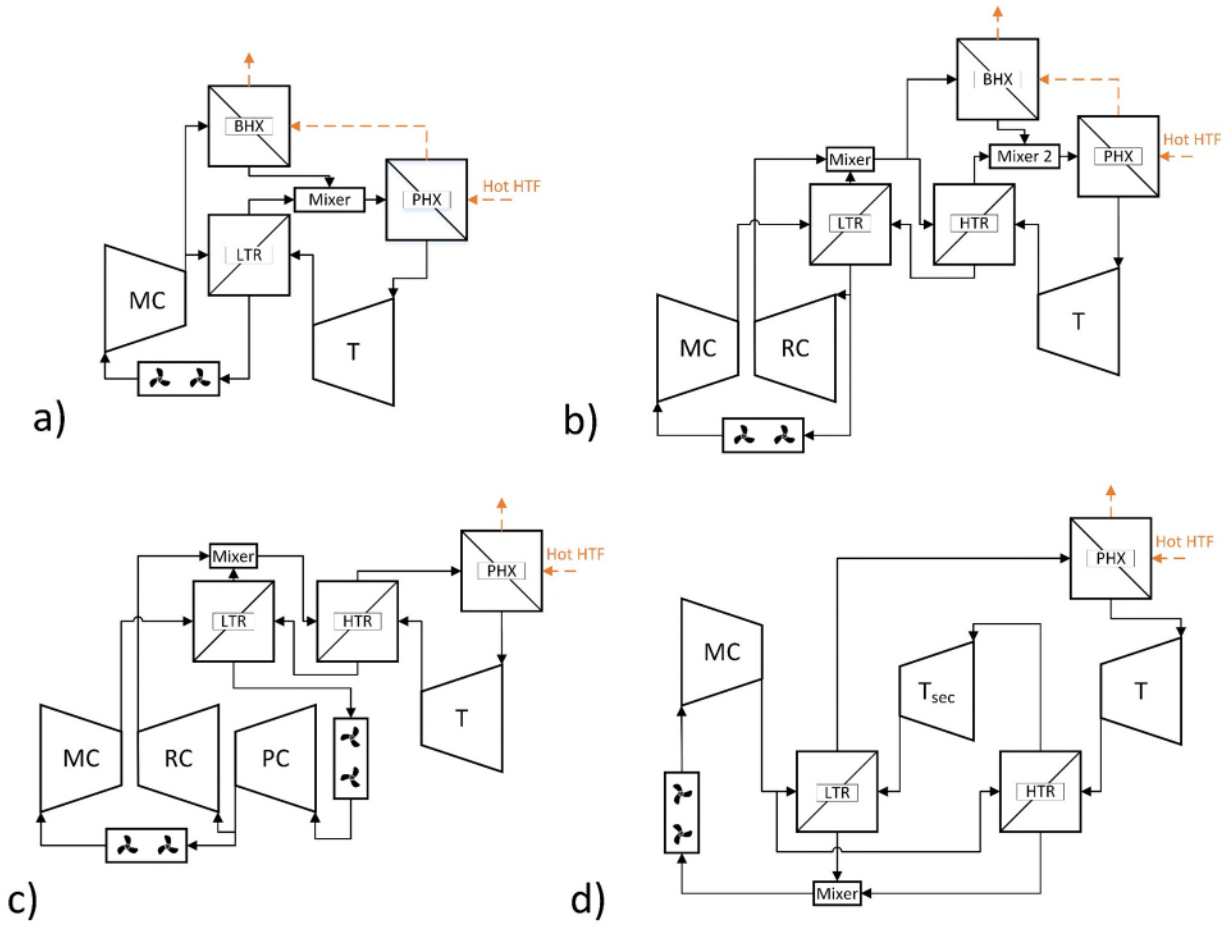

Figure 1. sCO_2 power cycle configuration schematics: a) simple cycle (with bypass), b) recompression cycle (with HTR bypass), c) partial cooling cycle, and d) turbine split flow cycle

We modeled four cycle configurations, shown in Figure 1. The simple, recompression, and partial cooling cycles present different trade-offs between complexity, efficiency, and HTF temperature difference. The turbine split flow cycle has been considered for waste heat applications and prioritizes HTF heat extraction which produces large HTF temperature differences. The models produce sub-configurations when certain components are removed, such as the removal of a recuperator if its assigned conductivity is zero, or removal of the recompressor if the recompression fraction is zero. The component costs come from Weiland et al. [7], except the PHX which is from Carlson et al. [8].

Table 1. sCO_2 power cycle parametric sweep free design variables.

Design Variable	Min	Max	N	Unit
Minimum Pressure	3.67	10.3	10	MPa
Intermediate Pressure Fraction	0	0.54	10	-
Recompression Fraction	0	0.23	10	-
Bypass Fraction	0	0.66	10	-
Turbine Split Fraction	0.389	0.54	10	-
Total recuperator conductance	0.1	2.27	10	MW/K
LTR/HTR conductance split	0	1	10	-

We performed a parametric sweep, which varied the free design parameters of each cycle over a range of 10 values, shown in Table 1. Every combination of each design variable value was simulated. We selected the bounds of the parametric sweep based on the range of optimal values in our previous work [3].

Each cycle design from the parametric sweep was used as an input to the CSP system model, which uses the cycle efficiency and HTF temperatures to design solar field, tower, receiver, and storage. The cycle model also calculates the parasitic losses due to particle conveyance. The falling particle receiver model is assumed to have a fixed thermal efficiency, based on preliminary results from a detailed receiver model. Key fixed parameters of the system and power cycle models are shown in Table 2.

Table 2. Key power and system fixed parameters.

Parameter	Value	Unit
Net Power	10	MWt
HTF	Bauxite [9]	
HTF Hot Inlet Temperature	775	°C
Ambient Temperature	30	°C
Air Cooler Approach Temperature	6	°C
Maximum Pressure	25	MPa
Solar Multiple	2.5	
Storage Duration	14	hr
Location	Daggett, CA	
DNI	950	W/m^2
Design Receiver Flux	1,400	kW/m^2
Receiver Efficiency	83	%
TES Height	47	m

The CSP system model produces the system specific cost (SSC) by dividing the total installed cost by the net power output, including parasitic losses.

RESULTS AND DISCUSSION

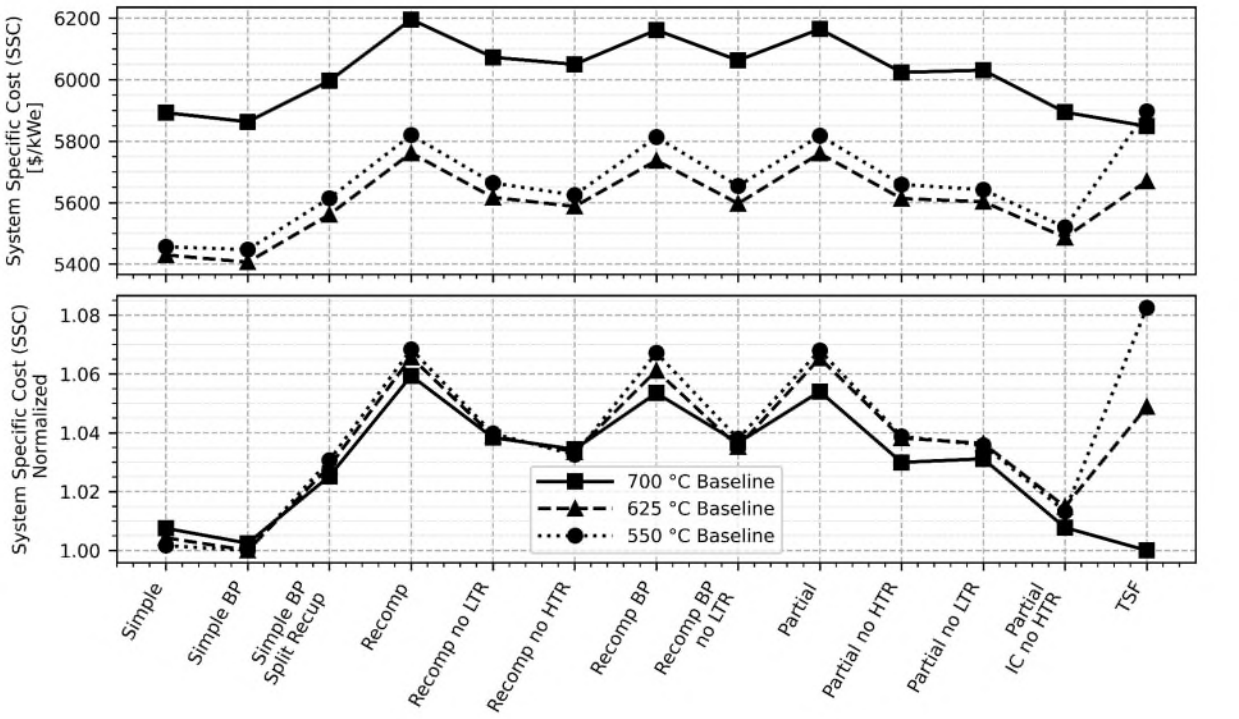

Figure 2. Baseline comparison of power cycle performance with various turbine inlet temperatures.

Figure 2 shows the impact of turbine inlet temperature on the system specific cost (SSC), by comparing the optimal cycle design for each configuration. The 625 and 550 °C cases display significant improvement compared to 700 °C, with a decrease of 7.8% and 7.1% in SSC, respectively, for the simple with bypass configuration. The normalized plot demonstrates how the optimal cycle configuration changes, with the simple with and without bypass strong at all temperatures, but the turbine split flow cycle becoming less optimal as the turbine inlet temperature decreases. The turbine split flow cycle's strong performance at high temperatures is partially due to the cycle employing separate hot and cold turbines, because the cold turbine operates at a lower temperature and is therefore less expensive. As the hot turbine inlet temperatures decrease for all configurations, the turbine split flow cycle's relative cost advantage from its cold turbine is nullified.

Generally, lowering the turbine inlet temperature decreases the thermal efficiency of the power cycle, but saves significant cost in the turbine and PHX, which overcomes the increased cost of the field and receiver required to overcome the reduced conversion efficiency. Because of the promising performance at lower temperatures, we expanded our sensitivity analysis by running all the sensitivity cases at the colder turbine inlet temperatures that were previously fixed at the baseline inlet temperature of 700 °C. Table 3 lists the parameters we varied in the sensitivity analysis.

Table 3. Sensitivity analysis design parameters.

Sensitivity Parameter	Unit	Baseline	Sensitivity Values	
PHX Cold Approach	°C	20	40	60
Turbomachinery Isentropic Efficiency (Compressor/Turbine)		85/90	80/90	80/85
Heliostat Cost	$/m^2	75	127	
PHX Cost Model		Carlson	Buck-low	Buck-high
Recuperator Cost		1x	0.5x	1.5x
TES Cost		1x	0.5x	1.5x

Cold Approach Temperature

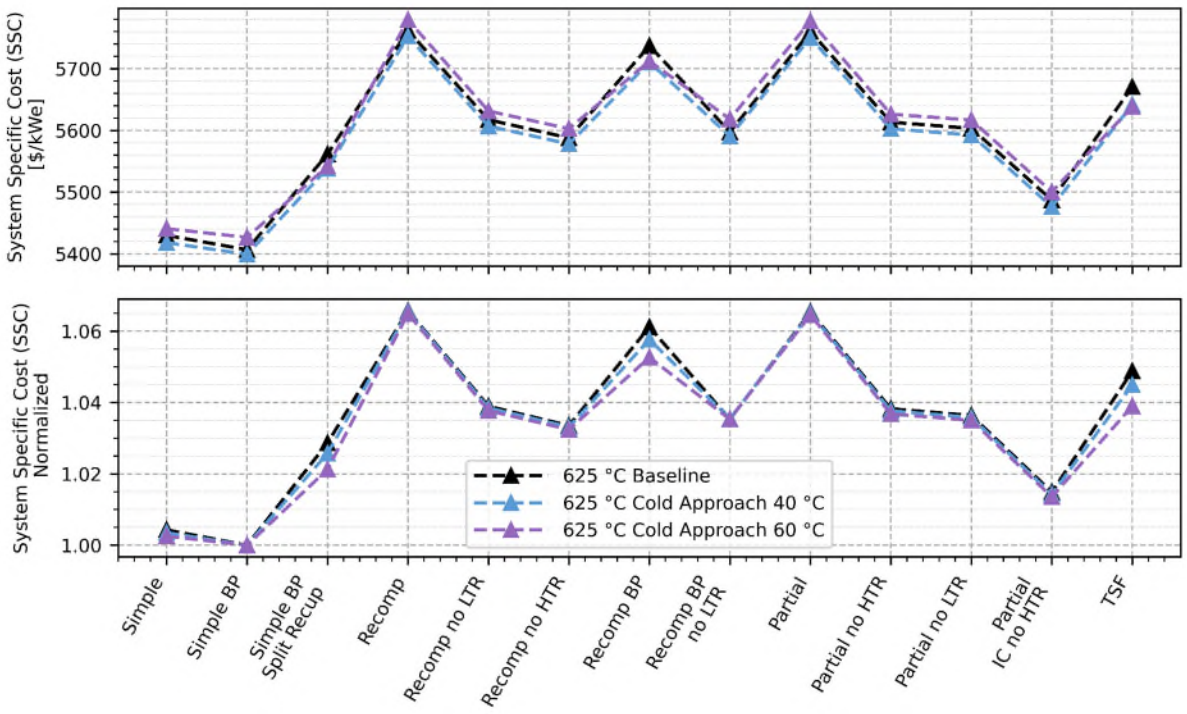

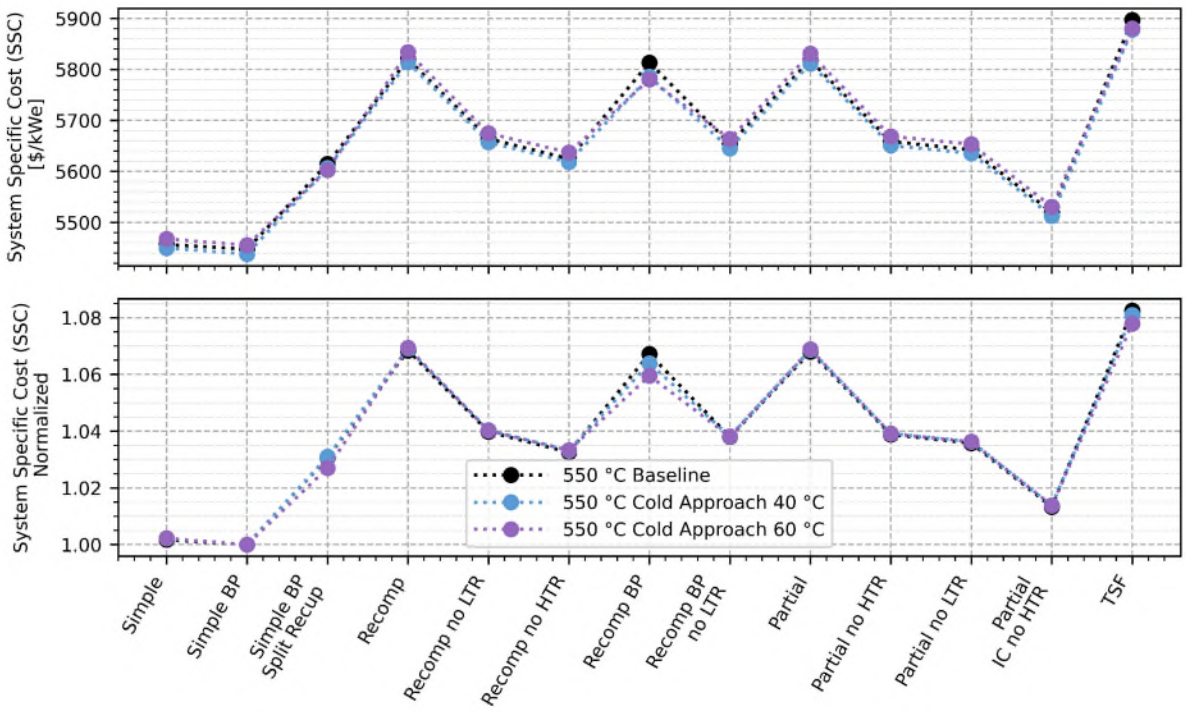

Figure 3. Cold approach sensitivity results for TIT of 625 °C (top) and 550 °C (bottom). The baseline cold approach temperature is 20 °C.

Figure 3 shows the effect of varying the PHX cold approach temperatures. The optimal configuration for both temperatures, the simple cycle with bypass, has a slight improvement using a cold approach temperature of 40 °C, with a decrease in SSC of 0.13% and 0.16% for the 625 and 550 °C cases, respectively. The sCO_2 temperature on the cold side of the PHX is calculated independently of the cold approach, so increasing the cold approach increases the HTF outlet temperature. This decreases the HTF temperature difference, but also decreases the cost of the PHX, because the required conductance is smaller. Varying the cold approach temperature does not meaningfully impact the selection of optimal configurations, as the simple with and without bypass are optimal at each cold approach temperature.

Turbomachinery Isentropic Efficiencies

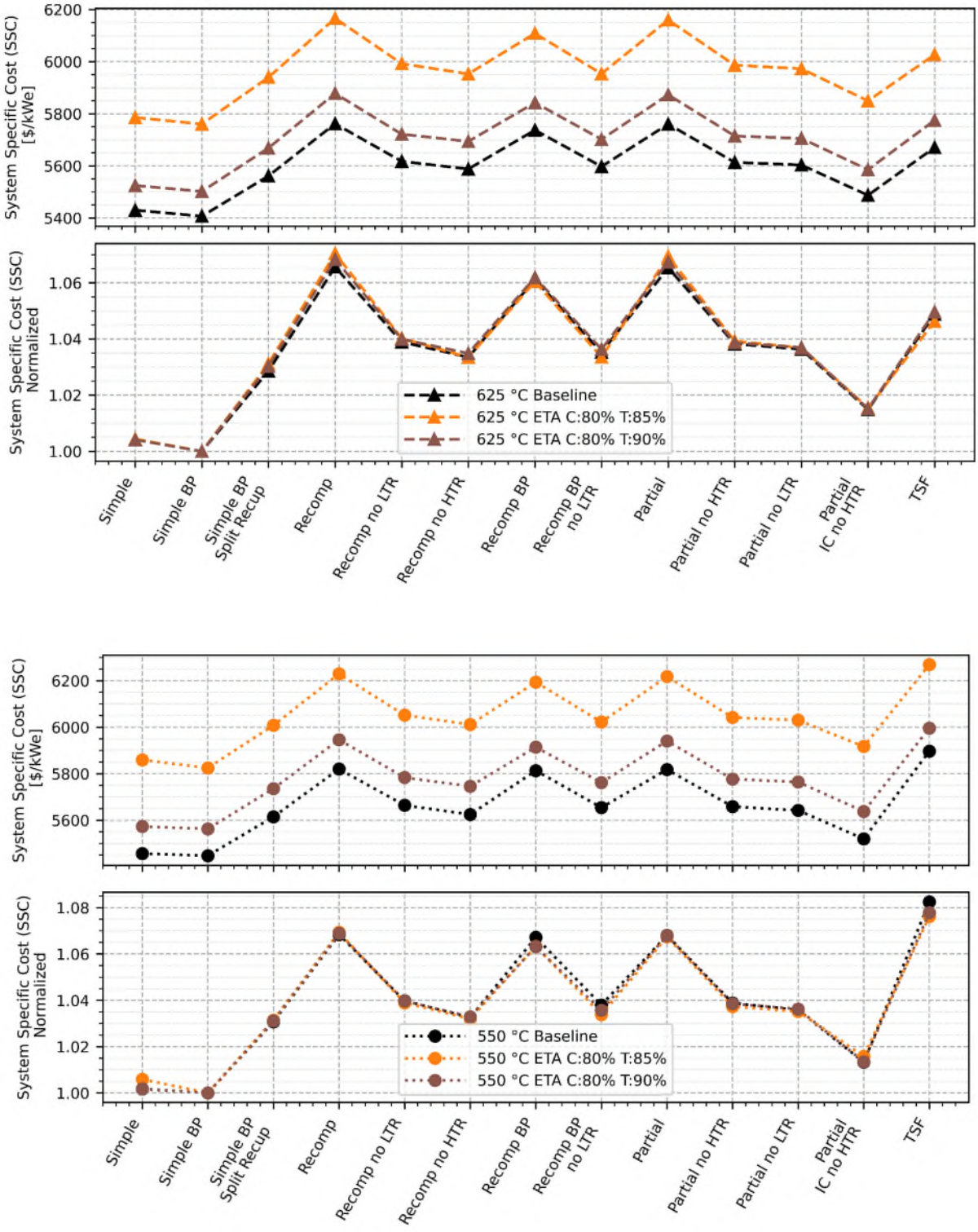

Figure 4. Turbomachinery isentropic efficiency results for TIT of 625 °C (top) and 550 °C (bottom). The baseline isentropic efficiency is 85% for compressors, 90% for turbines.

Figure 4 displays the performance of each configuration with varied turbomachinery isentropic efficiency. Decreasing the efficiency of the turbine and compressor naturally negatively impacts the overall performance. The case with the compressor efficiency of 80% and turbine efficiency of 85% increased the SSC of the 625 and 550 °C cases by 6.6% and 6.9%, respectively. The case with isentropic efficiencies of 80% and 90% for the compressor and turbine resulted in an increase of 1.8% and 2.1% for the 625 and 550 °C cases' SSC. The isentropic efficiency did not impact the optimal configuration, with the simple cycle with bypass being the optimal configuration in each case.

PHX Cost Model

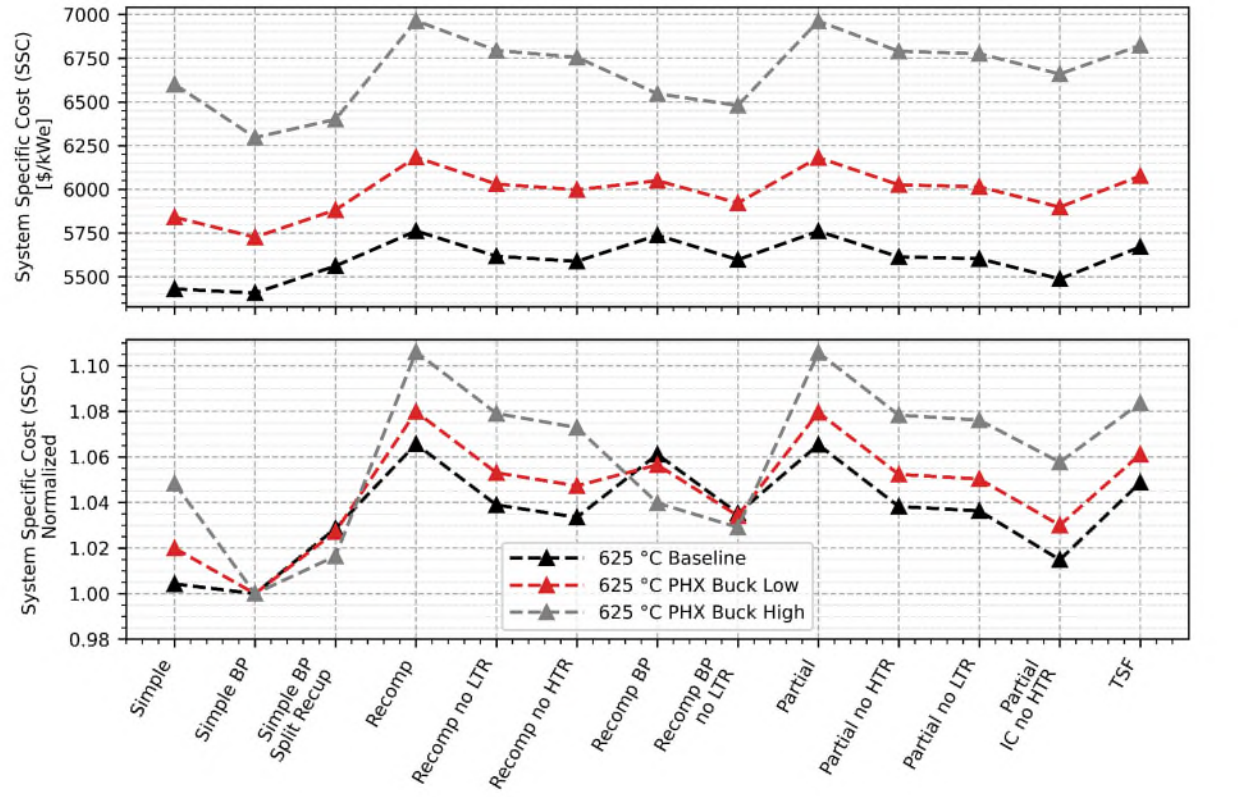

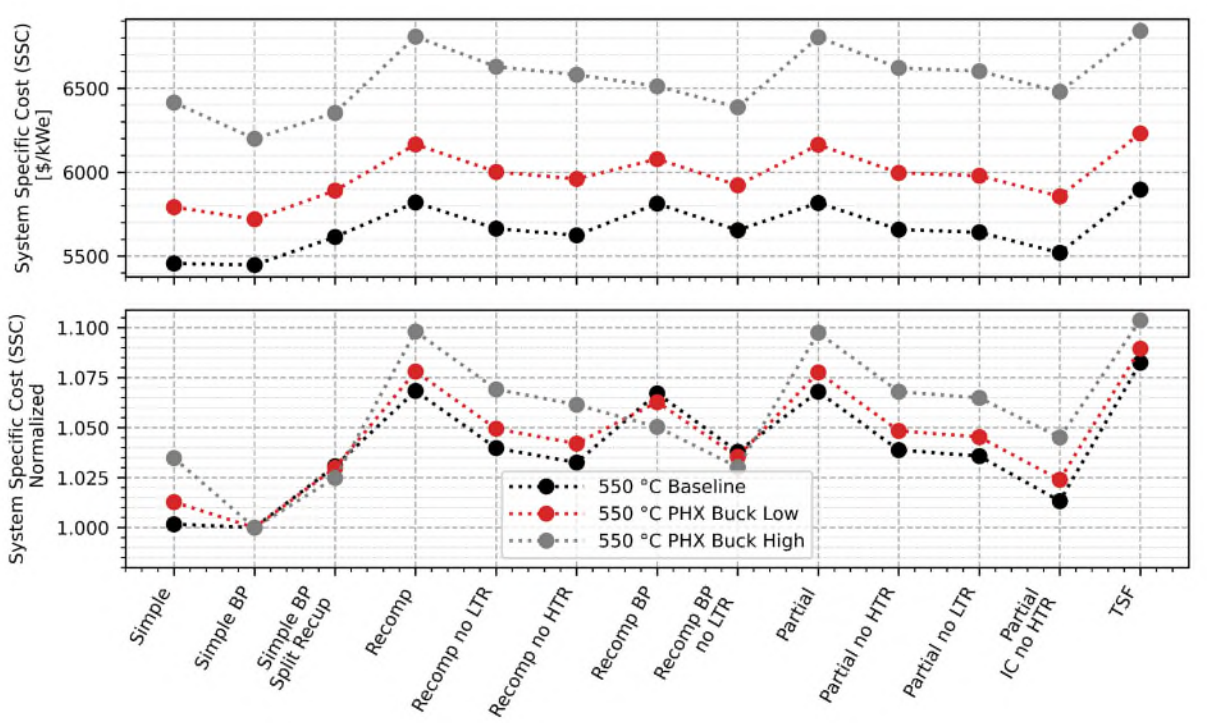

Figure 5. Varied PHX cost model results for TIT of 625 °C (top) and 550 °C (bottom).

We varied the PHX cost model by using the 'high' and 'low' cost models from Buck [10], which are for particles-to-sCO_2 heat exchangers. The Buck models are both higher cost than the baseline cost model from Carlson et al. [8] - the 'low' and 'high' models are 3.4x and 7.4x higher cost than the Carlson model, before inflation and assuming a particle convective coefficient of 350 W/m2-K. Figure 5 shows the impact of PHX cost on the SSC. For the optimal configuration, simple with bypass, the Buck low model increases the SSC by 5.9% and 5.0% for the 625 °C and 550 °C cases, respectively. The Buck high model increases the SSC by 16.5% and 13.8% for the 625 °C and 550 °C cases, respectively.

Both cases demonstrate the relative advantage of the bypass heat exchanger as the cost increases. The bypass heat exchanger takes a portion of the heat load away from the PHX, which decreases the cost of the PHX, and operates with larger approach temperatures, making the bypass heat exchanger (BHX) relatively less expensive. This is evident with the simple cycle: as the PHX cost increases, the simple cycle becomes less effective, and the cycles with bypasses increase their effectiveness.

Heliostat, Recuperator, and TES Cost

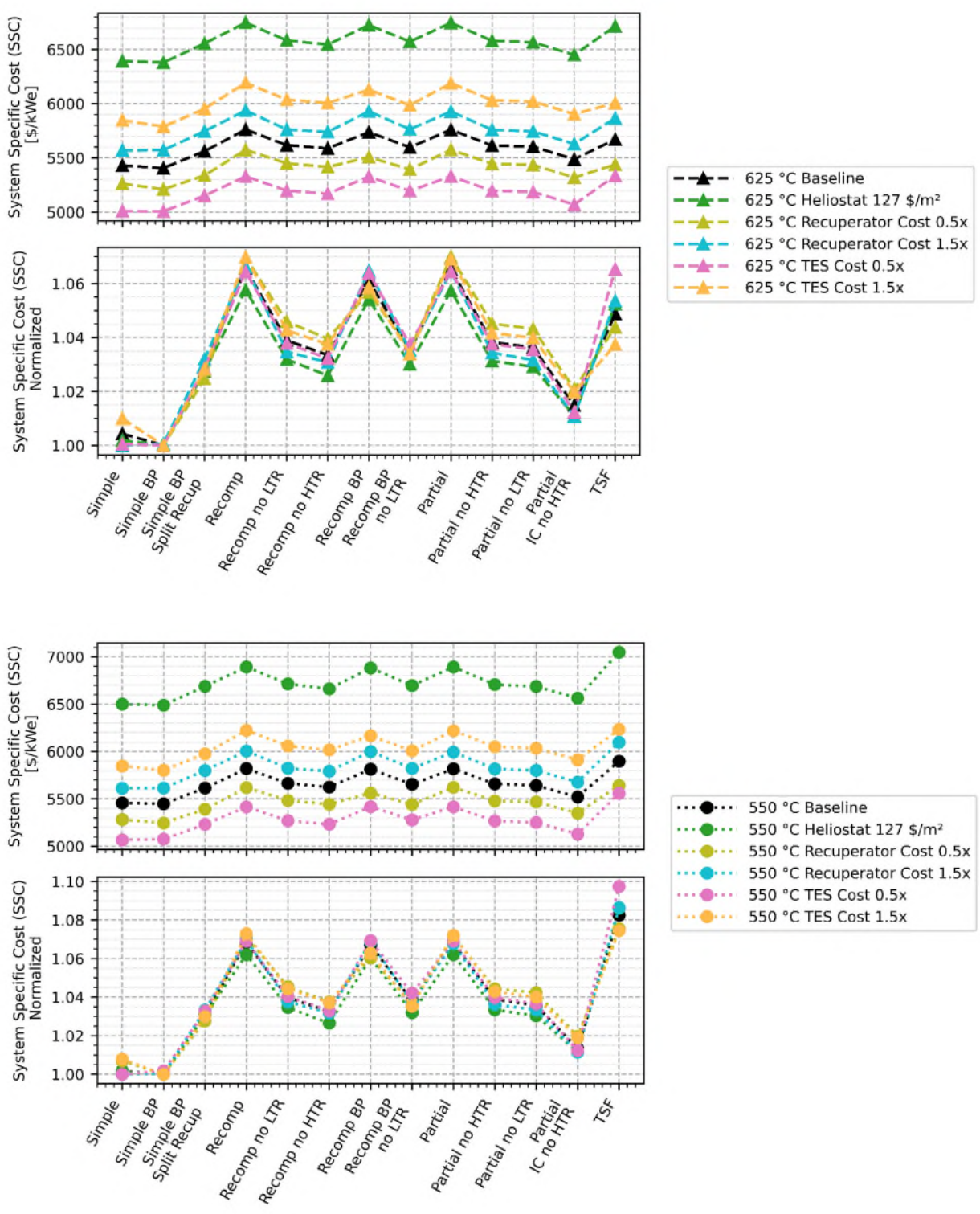

Figure 6. Performance results with varied heliostat, recuperator, and TES cost for TIT of 625 °C (top) and 550 °C (bottom). The baseline heliostat cost is 75 $/m2.

Figure 6 shows the performance with varied heliostat, recuperator, and TES cost. We set the heliostat cost to the 2025 System Advisor Model (SAM) [11] default value, 127 $/m2, compared to the baseline value of 75 $/m2. The increase results in an 18.0% and 19.1% increase in SSC for the 625 °C and 550 °C cases, respectively.

The storage cost also had a significant effect on performance, with a 7.4% and 7.0% decrease in SSC for the 0.5x case, and 7.1% and 6.5% increase for the 1.5x, for the 625°C and 550 °C cases, respectively. The recuperator cost effect was smaller than for storage, with a 3.6% and 3.7% decrease in SSC for the 0.5x case for 625 °C and 550 °C inlet temperatures, respectively, and 3.0% increase for both temperatures at 1.5x cost multiplier.

The normalized plot shows that the optimal configuration selection does not change significantly as the heliostat, TES, or recuperator costs change. For the case with higher TES costs, the simple cycle becomes less optimal than the simple with bypass cycle, because it has a smaller HTF temperature difference, which increases the size of TES. The simple bypass is also more optimal than the simple cycle when the recuperator cost is reduced, because the bypass cycle can increase the bypass fraction relative to baseline, which increases the HTF temperature difference, and overcome the expected loss in efficiency by increasing the recuperator conductance at low cost. For both temperatures, the simple with and without bypass cycles have similar efficiencies, but the bypass cycles have significantly larger HTF temperature differences when the recuperator cost is reduced.

10x Heliostat Cost

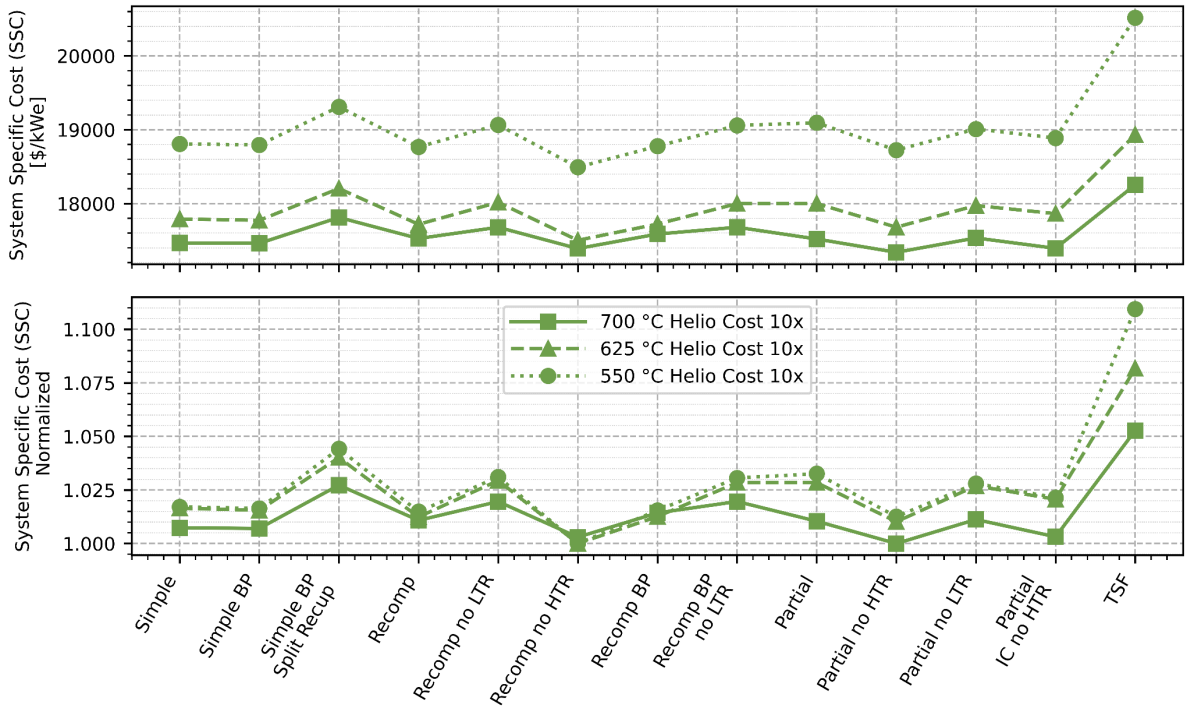

Figure 7. Comparison of cycle performance with 10x heliostat cost, for 700, 625, and 550 °C TIT. This data uses the expanded sweep bounds found in our previous work [3], with a maximum allowable recuperator conductance of 5 MW/K.

We also considered a special case with very high heliostat cost, 10x the baseline, to demonstrate

that high turbine inlet temperatures are optimal when the cost of heat is very high. For this case, we used the original, expanded sweep bounds from our previous work, with a maximum allowable recuperator conductance of 5 MW/K, because the cycles prioritize efficiency and require more recuperation. As shown in Figure 7, the 700 °C inlet temperature produces the lowest SSC - the 625 and 550 °C cases are 1.3% and 7.1% higher respectively. The optimal configuration is the partial cooling cycle for the 700 °C case, which has an efficiency of 49.0%. The 625 and 550 °C cases are optimal with the recompression cycle. Cycle thermal efficiency is the most important factor, because the cost of the field dominates the other costs in the system, so the optimal cases minimize the field size.

All Sensitivity Results

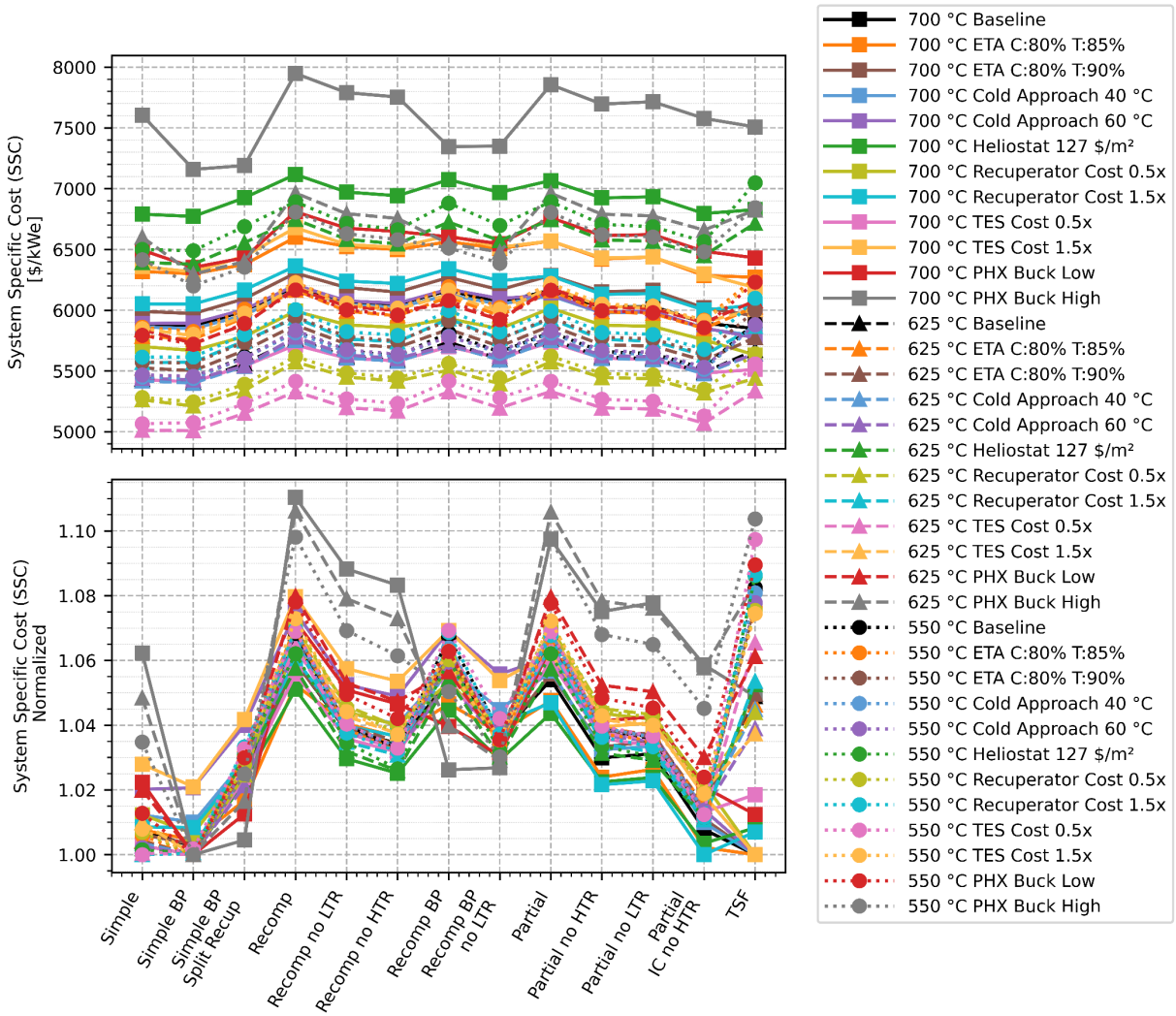

Figure 8. Optimal cases for each configuration for every sensitivity case.

Figure 8 compiles the results for every sensitivity case (except the heliostat cost 10x case), at each turbine inlet temperature. The normalized plot shows that the configurations designed for high efficiency, the recompression and partial cooling variants, are not optimal in any case presented. The turbine split flow cycle is optimal in half of the 700 °C cases but is not optimal in any case with a colder turbine inlet temperature. The simple cycle has strong performance

across the analysis but is less effective than its bypass counterpart for cases with high PHX or TES costs.

The simple cycle with bypass (Simple BP) is optimal in 21 out of the 24 cases with colder than 700 °C inlet temperatures, with an average SSC 0.01% higher than the relative optimal. The simple cycle with bypass benefits from the low complexity and cost associated with the simple cycle, with the added ability to increase the HTF temperature difference via BHX and economically split the heat load between the PHX and BHX, particularly in cases with high PHX costs.

CONCLUSION

This work models a 10 MWe falling particle CSP system with thermal energy storage and sCO_2 power cycle. We consider four cycle configurations: simple (with optional bypass), recompression (with optional bypass), partial cooling, and turbine split flow. The configurations have unique performance capabilities, from maximizing efficiency or HTF temperature difference, to minimizing cost or complexity. We perform a parametric sweep of cycle design variables and model each case in a CSP system design point model. The system model produces the system specific cost, which we use to compare cycle performance.

We lower the turbine inlet temperature from the baseline value of 700 °C and find the technoeconomic performance significantly improves with a decrease of 7.8 and 7.1% in the system specific cost for the 625 and 550 °C cases, respectively, for the simple with bypass cycle. The performance improvement is due to the cost savings in the turbine, PHX, and thermal energy storage, which make up for the decrease in cycle efficiency. We perform a sensitivity analysis at the lower temperatures to explore the impact of various design parameters on cycle performance and configuration selection.

The PHX cold approach temperatures and turbomachinery isentropic efficiencies have a minor impact on design selection and follow the impact trend seen at 700 °C. Increasing the PHX cost results in cycles with bypass being more effective, since the bypass cycles economically share the heat transfer with a lower cost bypass heat exchanger, taking some heat transfer away from the high cost PHX. We model a case with very high heat cost, with a 10x multiple on heliostat cost, to demonstrate when the high efficiency configurations with high turbine inlet temperatures are optimal. Overall, the turbine split flow cycle is only optimal in cases with high turbine inlet temperatures and the simple with bypass cycle is optimal in 21 out of 24 colder turbine inlet temperature cases.

REFERENCES

[1] Turchi, C. S., Ma, Z., Neises, T. W., and Wagner, M. J., 2013, “Thermodynamic Study of Advanced Supercritical Carbon Dioxide Power Cycles for Concentrating Solar Power Systems,” Journal of Solar Energy Engineering, **135**(041007). https://doi.org/10.1115/1.4024030.

[2] Albrecht, K. J., Bauer, M. L., and Ho, C. K., 2019, “Parametric Analysis of Particle CSP System Performance and Cost to Intrinsic Particle Properties and Operating Conditions,” *ASME 2019 13th International Conference on Energy Sustainability*, American Society of Mechanical Engineers, Bellevue, Washington, USA, p. V001T03A006. https://doi.org/10.1115/ES2019-3893.

[3] Brown, T., Neises, T., Hamilton, W., and Martinek, J., 2025, “Techno-Economic

Comparison of sCO2 Cycles for Particle-Based CSP at Design-Point Conditions," Solar Energy, **302**, p. 114034. https://doi.org/10.1016/j.solener.2025.114034.
[4] Alfani, D., Sobic, F., Astolfi, M., Binotti, M., and Silva, P., 2024, "Techno-Economic Analysis and Optimal sCO2 Power Cycle Configuration for Novel CSP Plants Adopting Tubular Fluidized Particles Central Receivers." https://doi.org/10.1115/GT2024-122779.
[5] Heller, L., Glos, S., and Buck, R., 2022, "Techno-Economic Selection and Initial Evaluation of Supercritical CO2 Cycles for Particle Technology-Based Concentrating Solar Power Plants," Renewable Energy, **181**, pp. 833–842. https://doi.org/10.1016/j.renene.2021.09.007.
[6] Heller, L., Glos, S., and Buck, R., 2026, "Cost Benefit Analysis of Supercritical CO2 Cycles in Next-Generation Solar Thermal Power Plants," Renewable Energy, **256**, p. 123613. https://doi.org/10.1016/j.renene.2025.123613.
[7] Weiland, N. T., Lance, B. W., and Pidaparti, S. R., 2019, "sCO2 Power Cycle Component Cost Correlations From DOE Data Spanning Multiple Scales and Applications," *Volume 9: Oil and Gas Applications; Supercritical CO2 Power Cycles; Wind Energy*, American Society of Mechanical Engineers, Phoenix, Arizona, USA, p. V009T38A008. https://doi.org/10.1115/GT2019-90493.
[8] Carlson, M. D., Middleton, B. M., and Ho, C. K., 2017, "Techno-Economic Comparison of Solar-Driven sCO2 Brayton Cycles Using Component Cost Models Baselined with Vendor Data and Estimates," *Proceedings of the ASME 2017 11th International Conference on Energy Sustainability*, Charlotte, NC, USA, pp. 1–7. https://doi.org/10.1115/ES2017-3590.
[9] 2025, "CARBOHSP," Carbo Ceramics. [Online]. Available: https://carbo.tech/products/carbohsp/. [Accessed: 15-Sept-2025].
[10] Buck, R., 2021, "G3P3 Techno-Economic Analysis of UpScaled CentRec® Receiver." [Online]. Available: https://elib.dlr.de/140177/. [Accessed: 12-Mar-2025].
[11] National Laboratory of the Rockies, 2024, "System Advisor Model™." [Online]. Available: https://sam.nrel.gov.

ACKNOWLEDGEMENTS

This work was authored by the National Laboratory of the Rockies for the U.S. Department of Energy (DOE) under Contract No. DEAC36-08GO28308. Funding provided by the U.S. Department of Energy Office of Critical Minerals and Energy Innovation Solar Energy Technologies Office. The views expressed in the article do not necessarily represent the views of the DOE or the U.S. Government. The U.S. Government retains and the publisher, by accepting the article for publication, acknowledges that the U.S. Government retains a nonexclusive, paid-up, irrevocable, worldwide license to publish or reproduce the published form of this work, or allow others to do so, for U.S. Government purposes.